Eur. Phys. J. B **61**, 309–318 (2008)
DOI: 10.1140/epjb/e2008-00080-6

THE EUROPEAN
PHYSICAL JOURNAL B

Electric field gradients in $PrBa_2Cu_3O_7$: LSDA+U results and comparison with experiment

V. Ghanbarian[1] and M.R. Mohammadizadeh[1,2,a]

[1] Superconductivity Research Laboratory (SRL), Department of Physics, University of Tehran, North Karegar Ave.,
P.O. Box 14395-547, Tehran, Iran
[2] Department of Nano-Science, Institute for Studies in Theoretical Physics and Mathematics (IPM),
P.O. Box 19395-5531, Tehran, Iran

Received 11 November 2006 / Received in final form 1st August 2007

Abstract. Electric-field gradient (EFG) and asymmetry parameter (η) at all oxygen and copper sites of nonsuperconducting $PrBa_2Cu_3O_7$ (Pr123) compound were calculated using the full-potential (linearized)-augmented-plane-wave plus local orbitals method. Exchange and correlation effects were treated by LSDA+U for Cu($3d$) and Pr($4f$) electrons. The effects of changing screened Coulomb parameters U_{Pr}, U_{Cu1}, and U_{Cu2} on the results were individually studied. The calculated EFG of O2 site is close to the EFG of O3 site at variance with the experimental result. It was shown that by increasing superconducting holes in O2 and O3 sites the EFG at these sites increase and vice versa. The most famous theories which have been proposed to explain the suppression of superconductivity in perfect (without any mis-substitution or other defects) Pr123 compound are not consistent with the experimental EFG at O2 and O3 sites. By replacing one Pr atom at the Ba site on unit cell of Pr123 (Pr_{Ba}), it was shown that Pr_{Ba} mis-substitution reduces the superconducting holes in both O2 and O3 sites and could be responsible for the suppuration of superconductivity in Pr123 samples. It is very probable that the unusual behaviors of experimental EFG at O2 and O3 sites of Pr123 are related to oxygen defects which are produced with Pr_{Ba} mis-substitution.

PACS. 74.25.Jb Electronic structure – 74.72.Bk Y-based cuprates – 71.15.Mb Density functional theory, local density approximation, gradient and other corrections – 76.60.-k Nuclear magnetic resonance and relaxation

Introduction

$PrBa_2Cu_3O_{7-\delta}$ is a unique compound in the $RBa_2Cu_3O_{7-\delta}$ (R = Y or a rare earth atom) system due to its singular behaviors [1]. All Pr123 samples that have been prepared by the conventional methods such as standard sintering procedure [2] show nonsuperconducting and nonmetallic behavior, in contrast to other $RBa_2Cu_3O_{7-\delta}$ samples. Some models have been proposed to explain this puzzling fact [1] but none of them has fully been accepted.

Self-consistent electronic structure calculations with local spin density approximation (LSDA) has already been performed for Pr123 using both the linear muffin tin orbitals with the atomic sphere approximation (LMTO-ASA) [3], and the full-potential-linearized augmented-plane-wave (FP-LAPW) method [4,5]. To overcome the failure of LSDA when describing strongly correlated systems, Biagini et al. [6] have reported the electronic structure calculations of Pr123 with the LSDA and on-site Coulomb interaction (LSDA+U) regime for only the Cu($3d$) electrons. Liechtenstein and Mazin have also calculated the electronic structure of Pr123 by taking into account the Coulomb correlations only for the Pr($4f$) electrons [7]. Qian et al. have included the correlation effects for both Cu($3d$) and Pr($4f$) electrons [8]. In all of the above LSDA+U calculations the LMTO method has been used (LMTO-ASA in [6–8] and FP-LMTO in [7]). Recently, we have also reported the band structure of Pr123 [9] with the full-potential (linearized)-augmented-plane-wave plus local orbitals (FP-(L)APW+lo) method using the LSDA+U.

In the LSDA [3–5] or when LSDA+U has been used only for Pr($4f$) orbitals [7,9], the CuO_2 planes of Pr123 show metallic character. In references [6,8,9] it has been indicated that the LSDA+U for Cu($3d$) orbitals largely enhances the insulating character of the CuO_2 planes in Pr123. All of the Pr123 samples that have been prepared by the conventional methods such as standard sintering procedure [2] show nonmetallic (and nonsuperconducting)

---

[a] e-mail: zadeh@ut.ac.ir

behavior in the CuO_2 planes [10]. Therefore, at first glance it seems that the LSDA+U calculations of references [6,8] for Pr123 are qualitatively perfect. Recently, some groups have claimed that using some unconventional methods, they have produced superconducting Pr123 samples [11, 12]. Moreover, some people argue that nonsuperconducting Pr123 samples are not perfect (mis-substitution or other defects) and perfect Pr123 samples should be superconductor and metal similar to Y123 [13–17]. In [9], we have shown that if we use LSDA+U for Pr($4f$) (with $U_{\mathrm{Pr}} \geqslant 0.3$ Ry) and use LSDA for all other atoms in Pr123 and Y123, the band structures of both systems would be the same. So, those calculations support the idea that perfect Pr123 sample should be metal and superconductor similar to Y123 compound and some impurities are responsible for suppression of superconductivity and metallic character of conventional samples.

In order to search which calculation in Pr123 is correct, we need to compare some key calculation results with some exact experimental data. The charge density is the most important key quantity in density functional theory (DFT) calculations [18,19] and the coincidence of it with experiment is the best evidence for correctness of calculated results. Detailed experimental charge density is needed to comparison with the calculated charge distribution. For such complicated materials such as Pr123, a detailed charge density cannot be obtained from X-ray diffraction data [20]. However, the electric field gradient (EFG) is ideally convenient for this purpose. The EFG at nuclear sites can be calculated directly from the self-consistent charge density without further approximation [20–23]. In particular, EFG is sensitive to the charge asymmetry around a specific site [22]. Moreover, EFG at the nuclear sites can be measured very accurately by NMR/NQR spectroscopy [24]. Except reference [5] in all of the self-consistent electronic structure calculations that have already been reported for Pr123 (Refs. [3–9]), the EFG values (or charge density) have not been reported. In this paper, we present the EFG and η at all oxygen and copper sites of nonsuperconducting Pr123 compound with FP-(L)APW+lo method using the LSDA+U for various sets of U_{Pr}, U_{Cu1}, and U_{Cu2} values. These results were compared with the experimental data.

Computational details

Present calculations were performed by the precise FP-(L)APW+lo method [25,26]. We have used WIEN2k code for this purpose [27]. The following muffin-tin radii: 2.80, 2.90, 1.80, and 1.65 a.u. were used for Pr, Ba, Cu, and O atoms, respectively. The plane-wave cutoff was chosen $R_{min}K_{max} = 7.5$ [20] and the wave function in the atomic region was expanded up to $l = 10$. The nonspherical part of the potential was expanded into spherical harmonics up to $L = 6$. The mixed LAPW/APW+lo basis set [25,26] was used; the APW+lo for all occupied l states of each atom and the LAPW for all other unoccupied l states. Using such combination of LAPW and APW+lo, smaller amount of $R_{min}K_{max}$ is required for accurate EFG calculation with respect to only LAPW basis set. Additional local orbitals (LO) were also used for all semicore states [28]. These LOs improve linearization and a consistent treatment of semicore and valance states would be possible in one energy window, and hence insure proper orthogonality [28]. About 2020 L/APW functions plus local orbitals (LO+lo) were used as basis set. This size of basis set is more than the values that have already been used [4,29].

The Brillouin-zone sampling in the self-consistent calculations was performed using 16 special k points in the irreducible Brillouin zone (IBZ). Calculations with 72 k points have yielded almost the same EFG results. The similar conclusion with 16 and 72 k points has also been confirmed in Y123 system [29]. The band states (valance+semicore) were treated in a scalar relativistic approximation and core states were treated full relativistically. The structural data of nonsuperconducting Pr123 sample was taken from reference [30]. All calculations were performed in ferromagnetic ordering for Pr and Cu atoms similar to references [3,4,6–9] rather than complex antiferromagnetic ordering that has been observed in experiments for Cu and Pr atoms [31]. We will discuss about the effects of this simplification in the results and discussion section.

The rotationally invariant scheme of LSDA+U that was defined by Liechtenstein et al. [32] used for Cu($3d$) and Pr($4f$) orbitals. For double-counting term of LSDA+U functional "around the mean field" (AMF) version was used [33,34] in all cases that were presented in Tables 1 and 2. In addition, some calculations were repeated using "fully localized limit" (FLL) [32,34] version to investigate the effects of different versions of double-counting term on results. For LSDA part the interpolation formula given by Perdew and Wang [35] was used. The U values for Pr($4f$) and Cu($3d$) orbitals were treated as the external parameters similar to [20,36]. For J values of Pr($4f$) and Cu($3d$) orbitals some fixed values were used which will be discussed in the next section.

Results and discussion

The EFG is a traceless symmetric tensor of rank 2, defined as the second derivative of the electrostatic potential (with respect to spatial coordinates) evaluated at the position of nucleus. As mentioned before, the EFGs at nuclear sites are calculated directly from the self-consistent charge density without further approximations [20–23]. Calculations indicate that the off-diagonal elements of the EFG tensor with respect to the unit cell axes a, b, and c vanish due to symmetries of Pr123 structure. By ordering the components V_{aa}, V_{bb}, and V_{cc} according to their magnitudes it is defined:

$$|V_{zz}| \geqslant |V_{yy}| \geqslant |V_{xx}| \, .$$

The EFG tensor is characterized by the largest component V_{zz} (in short EFG), and the anisotropy parameter η is defined as

$$\eta = (V_{xx} - V_{yy})/V_{zz},$$

Table 1. The calculated EFG (V_{zz}) in units of 10^{21} $\mathrm{V\,m^{-2}}$ at oxygen and copper sites of $PrBa_2Cu_3O_7$ for various sets of U and J values in Ry.

Case	J_{Pr}	U_{Pr}	J_{Cu1}	U_{Cu1}	J_{Cu2}	U_{Cu2}	Cu1	Cu2	O1	O2	O3	O4
1	0	0	0	0	0	0	5.9	−3	17.6	9.7	9.9	12
2	0	0.3	0	0	0	0	6.2	−5.2	17.9	12.7	12	12.1
3	0	0.5	0	0	0	0	6.3	−5.3	18	13.4	13.8	12.2
4	0	0.74	0	0	0	0	6.3	−5.3	17.9	13.4	13.3	12.2
5	0.05	0.74	0.1	0.25	0.1	0.25	6.3	−6.2	18.1	12.8	13.9	12.2
6	0.05	0.74	0.1	0.35	0.1	0.35	7.6	−10.7	17.4	12	12.7	11.8
7	0.05	0.74	0.1	0.55	0.1	0.55	−10.6	−16.6	17.1	10.2	10.9	11.4
8	0.05	0.74	0.1	0.75	0.1	0.75	−13.4	−20.3	15.5	9.5	10	10.2
9	0	0	0.1	0.45	0.1	0.45	7.9	−11.2	16.1	7.8	8.0	11.7
10	0.05	0.54	0.1	0.45	0.1	0.45	9.0	−14.9	17.8	10.7	10.8	12.1
11	0.05	0.74	0	0	0.1	0.55	6.4	−16.6	18.8	9.9	10.5	11.6
12	0.05	0.74	0.1	0.45	0.1	0.25	8.8	−6.2	17.1	12.5	13.2	12.1

Table 2. The calculated asymmetry parameter η at oxygen and copper sites of $PrBa_2Cu_3O_7$ for various sets of U and J values in Ry.

Case	J_{Pr}	U_{Pr}	J_{Cu1}	U_{Cu1}	J_{Cu1}	U_{Cu2}	Cu1	Cu2	O1	O2	O3	O4
1	0	0	0	0	0	0	0.4	0.1	0.4	0.1	0.1	0.3
2	0	0.3	0	0	0	0	0.5	0.1	0.4	0.3	0.1	0.3
3	0	0.5	0	0	0	0	0.5	0.1	0.3	0.3	0.2	0.2
4	0	0.74	0	0	0	0	0.5	0.1	0.3	0.2	0.2	0.2
5	0.05	0.74	0.1	0.25	0.1	0.25	0.3	0.0	0.3	0.3	0.3	0.2
6	0.05	0.74	0.1	0.35	0.1	0.35	0.7	0.0	0.4	0.3	0.2	0.2
7	0.05	0.74	0.1	0.55	0.1	0.55	0.9	0.0	0.5	0.4	0.3	0.3
8	0.05	0.74	0.1	0.75	0.1	0.75	0.7	0.1	0.5	0.4	0.4	0.3
9	0	0	0.1	0.45	0.1	0.45	1.0	0.0	0.5	0.2	0.2	0.4
10	0.05	0.54	0.1	0.45	0.1	0.45	0.9	0.0	0.4	0.3	0.3	0.3
11	0.05	0.74	0	0	0.1	0.55	0.6	0.0	0.4	0.4	0.3	0.2
12	0.05	0.74	0.1	0.45	0.1	0.25	0.9	0.1	0.4	0.3	0.2	0.3

where η varies between 0 (axial symmetry) and 1 ($V_{xx} = 0$).

The calculated EFGs and ηs for various O and Cu sites were given in Tables 1 and 2, respectively. The unit cell of Pr123 and the labeling of various atoms were also shown in Figure 1. There are two inequivalent copper sites in the unit cell of Pr123: one in the copper-oxide chains Cu1, and two in the two-dimensional CuO_2 layers Cu2. In addition, there are four inequivalent oxygen sites: one in the copper-oxide chains O1, four in the two-dimensional CuO_2 layers O2 and O3, and two in the bridging sites between the chains and planes O4. The calculations for Pr123 were performed in three different sets. In the first set (rows 1–4 of Tabs. 1 and 2), the U was applied only for Pr($4f$) orbitals and U_{Pr} parameter was treated as an external parameter. In [5], the EFG at Cu and O sites of Pr123 was calculated by FP-LAPW method using LSDA and a Pr valency of 4+ (3+) was simulated by treating the Pr($4f$) states as the localized states with a fixed occupation of 1 (2). We have used the LSDA for Cu sites in the first set of our calculations (rows 1–4 of Tabs. 1 and 2) similar to [5] to compare our results with it. In the second set (rows 5–8 of Tabs. 1 and 2), the U was applied for Pr($4f$) and Cu($3d$) orbitals. The parameter U_{Pr} was set to 0.74 Ry as has been used in [8] for Pr123 and kept fixed, but U_{Cu1} and U_{Cu2} were treated as external parameters. The values of U_{Cu1} and U_{Cu2} were chosen equal in all of this set of calculations. Finally, in the third set of calculations (rows 9–12 of Tabs. 1 and 2) we have performed some calculations for some specific goals which will be discussed in the following.

It must be mentioned that in some cases of the last set of calculations U_{Cu1} was selected different from U_{Cu2}. Since Cu1 and Cu2 have different environments in R123 crystals, due to some reasons such as screening effects in solids [37], U_{Cu1} and U_{Cu2} can be selected different. For example in some calculations of [20], which have been performed for Y123, U_{Cu1} and U_{Cu2} were selected very different ($U_{\mathrm{Cu1}} = 0$ and $U_{\mathrm{Cu2}} = 0.59$ Ry). In addition, in [38] for calculation of electronic structure of the 1×1 Y123/Pr123 superlattice, U_{Cu} (=0.48 Ry) has been used only for Cu2 in Pr123 but the zero U value has been used for Cu1 in Pr123 and for all Cu atoms in Y123.

In all of the cases that LSDA+U has been used for Pr or Cu atoms, the parameters J_{Pr} and J_{Cu}, were set to usual Pr and Cu values of 0.05 Ry [8] and 0.1 Ry [8,33], respectively except the cases 1–4 that J_{Pr} was set to zero for simplicity. In Table 3 it is shown that the variation of J_{Pr} has only a minor effect on the EFG of Cu and O sites. So, there is no considerable error in selecting zero value for J_{Pr} rather than 0.05 Ry. The U and J values for $3d$ states of an atom are related to the screened

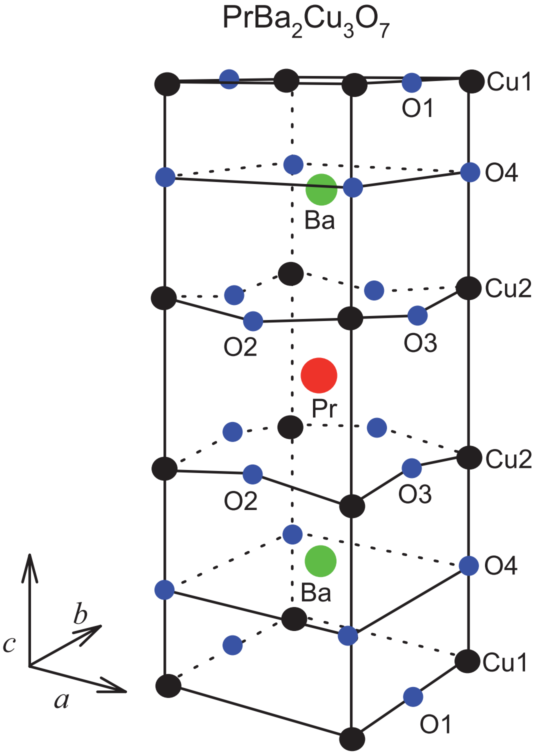

Fig. 1. The unit cell of Pr123 compound.

Table 3. The calculated EFG (V_{zz}) in units of 10^{21} V m^{-2} at oxygen and copper sites of $PrBa_2Cu_3O_7$ for $J_{Pr} = 0$ and $J_{Pr} = 0.05$ Ry. $U_{Pr} = 0.74$ Ry in both calculations.

Case	Cu1	Cu2	O1	O2	O3	O4
$J_{Pr} = 0$	6.3	−5.3	17.9	13.4	13.3	12.2
$J_{Pr} = 0.05$ (Ry)	6.2	−5.2	17.7	13.7	13.7	12.3

Coulomb integrals F^k [33,37]. For 3*d* states $U = F^0$ and $J = (F^2 + F^4)/14$ [33]. Screening effects in solids can considerably change F^0 and therefore U value for 3*d* states of an atom such as Cu [37]. Therefore, one U_{Cu} value that is convenient for a specific compound may not be convenient for another. In spite of this, screening effects in solids do not largely influence F^2 and F^4 from individual atomic values (atom outside the solid) [37]. So, the J value of 3*d* orbitals of an atom such as Cu is not largely changed from one solid to another. Therefore, we have not used J_{Cu} value as an external parameter and fixed it at 0.1 Ry which, has already been used in references [8,33].

In the first set of our calculations we study the effects of U_{Pr} on EFGs and ηs. In the cases 1–4 in Table 1, the U was implemented only for Pr(4*f*) orbitals. Table 1 indicates that with increasing U_{Pr} from zero to the larger values, the absolute value of the EFG at all sites increases. (Note that after this, the words "absolute value" is dropped for simplicity.) The increment of the EFGs is nonlinear with respect to the U_{Pr} and the saturation was found for the larger U_{Pr}. The enhancement of EFG for Cu2, O2, and O3 sites is very larger than Cu1, O1, and O4 sites. Especially, the EFG in Cu2 site for $U_{Pr} = 0.74$ Ry is about 77% larger than the corresponding one for $U_{Pr} = 0$ Ry (i.e. LSDA), while for Cu1 is about 7%. So, the effect of U_{Pr} on the CuO_2 planes is very larger than the CuO chains. Increment of U_{Pr} has not very large effects on ηs, especially for Cu2 sites. In addition, the saturation behavior of η was found similar to the EFG cases.

Table 4. The EFG (V_{zz}) in units of 10^{21} V m^{-2} at oxygen and copper sites of $PrBa_2Cu_3O_7$ which has been calculated in reference [5].

Case	Cu1	Cu2	O1	O2	O3	O4
4+	6.1	0.6	17.2	8.3	8.3	11.6
itinerant	6.5	−2.5	17.8	9.4	9.8	12.0
3+	7.0	−5.6	17.8	13.1	13.7	11.7

The EFG at Cu and O sites of Pr123 has been calculated with FP-LAPW method using the LSDA in [5]. In this reference three calculations have been performed; Pr^{3+}, itinerant, and Pr^{4+}. In itinerant case the Pr(4*f*) electrons have been included as the band states (similar to all of our calculations), while in Pr^{4+} (Pr^{3+}), Pr valency of 4+ (3+) has been simulated by treating the Pr(4*f*) states as localized states with a fixed occupation of 1 (2). In this reference, the antiferromagnetic ordering has been used only for Pr atoms and the antiferromagnetic ordering of Cu atoms ignored. The calculated EFG and η in reference [5] were collected in Tables 4 and 5 for comparison with our results. The EFG and η at Cu and especially O sites of our LSDA calculation (case 1 in Tabs. 1 and 2) are reasonably close to itinerant case in Tables 4 and 5. Some small differences between our results and reference [5] may correspond to the differences in computational parameters or methods (such as using (L)APW+lo and LO basis set in our calculation rather than old LAPW which have been used in [5]). Another source of the mentioned discrepancies could be due to the difference in magnetic ordering of Pr atoms; we have used ferromagnetic ordering for Pr while in reference [5] antiferromagnetic ordering have been used. Such differences in the EFG results have already been reported in Y123 which is not a magnetic compound. For example, the calculated EFG at Cu1 site of Y123 is 6.9×10^{21} V m^{-2} [29], 7.4×10^{21} V m^{-2} [22], and 6.1×10^{21} V m^{-2} [39]. In spite of using the ferromagnetic ordering of Pr in the present work, the EFG and η at O sites were not almost affected in comparison with the antiferromagnetic ordering results [5]. It is important evidence that when we would study the EFG at nonmagnetic O sites the magnetic ordering of Pr is not important and we can use ferromagnetic ordering for Pr rather than antiferromagnetic ordering.

When we use U_{Pr} and increase it from zero (case 1) to 0.74 Ry (case 4) the EFG of all Cu and O sites increases and it almost approaches to the case 3+ and gets far from the case 4+ in Table 4. So, by using the LSDA+U for Pr(4*f*) states the valency of Pr gets near to 3+ value. Various techniques including inelastic neutron-scattering [40,41] and NMR experiments [42,43] show that

Table 5. Asymmetry parameter (η) at oxygen and copper sites of $PrBa_2Cu_3O_7$ which has been calculated in reference [5].

Case	Cu1	Cu2	O1	O2	O3	O4
4+	0.6	0.3	0.3	0.2	0.3	0.2
itinerant	0.6	0.2	0.4	0.2	0.2	0.2
3+	0.7	0.1	0.3	0.3	0.3	0.1

Table 6. The experimental EFG (V_{zz}) in units of 10^{21} V m^{-2} and asymmetry parameter η at Cu sites of nonsuperconducting Pr123. The values corresponding to Cu1 and Cu2 were taken from [44,45] and [44], respectively.

	Cu1	Cu2
EFG [44]	± 8.2	∓ 6.7
η [44]	—	0.0
EFG [45]	± 7.9	—
η [45]	0.9 ± 0.1	—

Table 7. The experimental EFG (V_{zz}) in units of 10^{21} V m^{-2} and asymmetry parameter η at oxygen sites of nonsuperconducting $PrBa_2Cu_3O_{7-\delta}$, $YBa_2Cu_3O_{7-\delta}$, and $YBa_2Cu_3O_{6.6}$. In the conversion from frequency unit to 10^{21} V m^{-2} units the quadrupole moment $Q = -0.026$b for ^{17}O [59] has been used.

		O1	O2	O3	O4
$PrBa_2Cu_3O_{7-\delta}$ [46]	EFG	—	6.9	10.2	11.1
	η	—	0.09	0.40	0.24
$YBa_2Cu_3O_{7-\delta}$ [24]	EFG	17.3	10.5	10.2	11.6
	η	0.41	0.21	0.24	0.32
$YBa_2Cu_3O_{6.6}$ [51]	EFG	—	9.4	9.4	11.0
	H	—	0.23	0.23	0.29

the valency of Pr is close to +3. In addition, experimental EFG and η at Cu1 and Cu2 sites of nonsuperconducting Pr123 samples [44,45] were collected in Table 6. By comparing the EFG and η values at Cu1 and Cu2 sites of cases 1–4 with the experimental values (Tab. 6), we understand that with increasing U_{Pr} from zero (LSDA) to 0.74 Ry, the EFG at Cu sites is improved. In spite of it, the main problem is related to O sites. The EFG at O2, O3, and O4 sites of nonsuperconducting Pr123 samples have been reported by ^{17}O NMR spectroscopy in [46]. The experimental EFGs and ηs at oxygen sites were collected in Table 7. By comparing the EFG values at O sites of cases 1–4 with the experimental data (Tab. 7), we understand that with increasing U_{Pr} from zero to 0.74 Ry, the calculated values deviate from the experimental data.

In the second set of our calculations, the parameter U_{Pr} was fixed at 0.74 Ry as has been used in reference [8] for Pr($4f$). This is near to the value (0.81 Ry) that has been used for La($4f$) [33]. It must be mentioned we do not claim that the value 0.74 Ry is the best value for U_{Pr}. We have fixed U_{Pr} value at 0.74 Ry since we would like to study the effects of U_{Cu} on the results. The EFGs of all sites approximately change linearly with respect to the U_{Cu} ($= U_{\mathrm{Cu1}} = U_{\mathrm{Cu2}}$) without saturation, at least up to $U = 0.75$ Ry. The EFG of Cu1 and Cu2 sites increases very largely with increasing U_{Cu}. The sign of EFG in the Cu1 site was changed due to changing the orientation of the EFG from V_{bb} to V_{aa} in the larger U_{Cu}. The EFG at all O sites reduces with increasing U_{Cu}. It is interesting that the EFG of O2 increases from 9.7×10^{21} V m^{-2} to 13.4×10^{21} V m^{-2} with increasing U_{Pr} from zero to 0.74 Ry (see rows 1–4). However, it decreases from this value (9.7×10^{21} V m^{-2}) to 9.5×10^{21} V m^{-2} with increasing U_{Cu} from zero to 0.75 Ry. Moreover, there is a similar behavior for O3 site. So, the effects of increasing U_{Cu} and U_{Pr} (from zero to about 0.75 Ry) on oxygens of CuO_2 plane are in the same order of magnitude, but in reverse direction. In contrast, both U_{Pr} and U_{Cu} enhance the EFG at Cu2 site although the effect of U_{Cu} is larger than U_{Pr} on Cu2 site. Table 2 shows that the η at Cu1 was enhanced very largely by changing U_{Cu} in contrast to the η at Cu2. The η at O2, O3, and O4 atoms shows a small increment with increasing U_{Cu}, but η at O1 atom is more affected.

Some other calculations were performed and reported in rows 11 and 12 of Tables 1 and 2 with $U_{\mathrm{Cu1}} \neq U_{\mathrm{Cu2}}$. They belong to the third set of our calculations. For a fixed U_{Pr}, the EFG and η of Cu1 almost depend only on the U_{Cu1} and the EFG and η of Cu2 almost depend only on the U_{Cu2}. For example, comparison of the EFG of Cu sites in case 11 with case 7, case 12 with case 5, and case 11 with case 4 makes it more clear. So, for a fixed U_{Pr}, it is possible to estimate U_{Cu1} and U_{Cu2} such that the experimental values of EFGs of Cu1 and Cu2 would be produced. For example, in case 12, the U_{Pr} was selected equal to 0.74 Ry and the U_{Cu1} and U_{Cu2} were estimated such that the experimental values of EFG and η of Cu1 and Cu2 sites (Tab. 6) were almost produced. We can not claim that the case 12 is the best unique calculation. Comparison between the case 12 and Table 7 shows that the calculated EFG at O3, O4, and especially O2 sites are larger than the experimental values. So, the results of case 12 are not consistent with the experiment. With decreasing U_{Pr} and increasing U_{Cu1} and U_{Cu2} simultaneously, the EFG of Cu1 and Cu2 sites would be fixed close to the experimental values while, the EFG of O2, O3, and O4 sites decrease and approach to the experimental values. More investigations show that with this technique we may be able to adjust the EFG of Cu1, Cu2, O3, and O4 sites simultaneously very close to the reported experimental data but, for O2 site seems impossible. All of the calculations that were reported in Tables 1 and 2 and many other calculations that we have performed with different values of U_{Pr}, U_{Cu1}, and U_{Cu2} (which were not reported in Tabs. 1 or 2) show that the calculated EFG at O2 site is close to the EFG at O3 site at variance with the experimental finding that the EFG at O2 site is dramatically smaller than at O3 site.

We try to find out the main reason of this discrepancy and discuss about the various possibilities. Mainly five reasons could be responsible for this discrepancy; (a) low convergence in the self-consistent calculations; (b) dependence of the calculated EFG on the lattice parameters; (c) simple ferromagnetic ordering that was used rather than the experimentally observed antiferromagnetic ordering [31]; (d) failure of the LSDA+U to produce unusual complex charge distribution of Pr123 system; (e) some shortcomings in the experimental EFG results, probably due to defects in the nonsuperconducting Pr123 samples.

The degree of convergence in the (L)APW+lo calculations mainly depends on the number of k points in the IBZ, on the LM combinations and Fourier coefficients in the expansion of potential and charge density, and the number of plane waves in the (L)APW+lo basis. Variations of fixed parameters that were specified in the computational details (such as number of k points, $R_{min}K_{max}$,...) show that our EFG results are reliable at least to about 10% and η to about 0.1 error. So, low convergence can not be responsible for this discrepancy that the calculated EFG at O2 site is close to the EFG at O3 site at variance with the experimental finding.

Carefully prepared Y123 and also Pr123 samples by conventional methods show very close structural parameters to each other. In [47] the effects of using slightly different structural parameters on the EFGs of Y123 have been investigated; it has been shown that using slightly different structural parameters shifts the EFG at O2 and O3 sites less than 2.4%. Similar to Y123 case, using different experimental structural parameters for conventional-prepared (nonsuperconducting) Pr123 samples, it is not expected the discrepancy with experimental data would be removed. As mentioned in the introduction, some groups have recently claimed that using some unconventional methods, they have produced superconducting Pr123 samples [11,12]. The lattice parameters of superconducting Pr123 crystals are slightly different from piece to piece and the atomic positions on these samples have not been reported [11]. However, in the entire superconducting samples, the c lattice parameter is longer than the c of the conventional nonsuperconducting samples [11], and is near to the value predicted by the c lattice parameter vs. RE^{3+} ionic radii curve for the RE123 superconducting compounds [30,48]. In reference [9], we have used the structural parameters corresponding to Pr^{3+} in RE123 curves of reference [48] for calculation of the band structure of superconducting Pr123 samples. Although, the structural parameters of Pr123 which have been predicted from RE123 curves [48], are very different from the structural parameters of the conventional nonsuperconducting Pr123 samples [48], the calculated band structures from these two different structural parameters are very similar, qualitatively [9]. In addition, we have tested that using these two different structural parameters the EFG at O2 and O3 sites shift less than 4.2% and the EFG at O2 site is almost equal to the EFG at O3 site for both structural parameters.

It has been mentioned by Singh [4] and Biagini et al. [6] that the magnetic ordering of ions is expected to contribute in energy a little with respect to the band energies. So, it does not affect the charge balance between the various components of the crystal, significantly. So, they have performed their calculations for Pr123 in simple ferromagnetic ordering rather than experimentally reported antiferromagnetic ordering [31]. In above, we indicated that the magnetic ordering of Pr has not any considerable effects on the EFG at Cu and especially O sites. So, we have used ferromagnetic ordering for Pr rather than antiferromagnetic ordering. The Pr123 compound has shown very complex noncollinear antiferromagnetic ordering in low temperatures (below 20 K) [31]. Very huge supercell is needed for simulation of antiferromagnetic ordering of Cu atoms. So, we ignore the antiferromagnetic ordering in Cu atoms in our present calculations. The complex antiferromagnetic ordering of Cu atoms [31] may be important for investigating the EFG at Cu sites but it has low importance in O atoms sites which are nonmagnetic. Investigating the reason(s) of discrepancy between the calculated EFG at O2 and O3 sites with the experimental data is our main goal here. So, using ferromagnetic ordering for Cu atoms is not produced serious problem.

In reference [20] the effects of various versions of double-counting term on the EFG at Cu sites of some cuprates have been investigated. Using reference [20] results and some calculations that we have performed with FLL version [32,34], it was cleared that for producing the same EFG at the Cu site using different versions of double-counting term, various amounts of U_{Cu} are required. However, we have tested that the FLL version for double-counting term produces the EFG at O2 site almost equal to the EFG at O3 site, similar to the AMF version. The FLL and AMF are two limiting approximations for double-counting term [34]. Therefore, using the other versions of double-counting term that have been suggested from interpolation between these two limiting cases [20,34], it does not seem that the large discrepancy between experimental and calculated EFG at O2 and O3 sites would be removed. However, the LSDA+U is an approximation and it may not contain all strong-correlation effects in the Pr123 complex system. So, the discrepancy between our calculations and the experimental EFG at O sites may be related to failure of the LSDA+U approach. There are some other methods for investigating strongly correlated systems such as LDA+SIC (Self-Interaction Corrections), OEP (Optimized Effective Potential method) and GW approximation [49]. These methods could also be tested in Pr123 in other independent works.

Table 8. The O2(p) partial charges of Pr123 corresponding to the first set of calculations.

U_{Pr}(Ry)	p_x	p_y	p_z
0.00	1.105	1.267	1.248
0.30	1.070	1.300	1.257
0.50	1.059	1.309	1.258
0.74	1.060	1.303	1.262

Table 9. The O3(p) partial charges of Pr123 corresponding to the first set of calculations.

U_{Pr}(Ry)	p_x	p_y	p_z
0.00	1.266	1.097	1.248
0.30	1.285	1.071	1.262
0.50	1.306	1.052	1.262
0.74	1.301	1.058	1.262

Table 10. The $O2(p)$ partial charges of Pr123 corresponding to the second set of calculations.

$U_{\mathrm{Cu1,2}}$(Ry)	p_x	p_y	p_z
0.25	1.072	1.303	1.255
0.35	1.087	1.301	1.255
0.55	1.115	1.299	1.250
0.75	1.134	1.299	1.250

Table 11. The $O3(p)$ partial charges of Pr123 corresponding to the second set of calculations.

$U_{\mathrm{Cu1,2}}$(Ry)	p_x	p_y	p_z
0.25	1.304	1.063	1.262
0.35	1.302	1.075	1.260
0.55	1.298	1.105	1.255
0.75	1.296	1.123	1.252

The partial charge p_x, p_y, and p_z of O2 and O3 atoms for the first (second) set of our calculations are collected in Tables 8 and 9 (10 and 11), respectively. In Tables 8–11, the small amount of $O2(p_x)$ and $O3(p_y)$ partial charges in comparison with the other O2(p), and O3(p) partial charges is related to the pdσ-antibonding hybridization characteristic $Cu2(d^2_{x-y}{}^2)$-$O2(p_x)$-$O3(p_y)$ of the R123 cuprates [9,22]. Decrease of the occupation number of $O2(p_x)$ (that is named $O2(p_\sigma)$) and $O3(p_y)$ (that is named $O3(p_\sigma)$) orbitals is interpreted as the creation of holes with p_σ characters. By simultaneous study of Tables 1 and 8–11 we understand that with increasing the $O2(p_\sigma)$ ($O3(p_\sigma)$) holes (decreasing $O2(p_x)$ ($O3(p_y)$) electrons), the EFG at O2 (O3) site increases and vice versa. Except some people [13–17], the majority of people believe that pdσ holes in the CuO_2 planes of R123 cuprates participate in superconductivity. So, the EFG values at O2 and O3 sites contain important information about superconducting holes.

The number of superconducting holes of $YBa_2Cu_3O_7$(which have $O2(p_\sigma)$ and $O3(p_\sigma)$ characters) are larger than the corresponding one in $YBa_2Cu_3O_{6.6}$ compound [50]. In addition, the experimental amount of EFG at O2 and O3 sites in $YBa_2Cu_3O_7$ [24] is also larger than in $YBa_2Cu_3O_{6.6}$ [51] (Tab. 7). These observations confirm our theoretical claim that with increasing the superconducting $O2(p_\sigma)$ ($O3(p_\sigma)$) holes, the EFG at O2 (O3) site increases and vice versa. The experimental EFG at O2 site in $YBa_2Cu_3O_7$ is almost equal to O3 site (Tab. 7) and it is in agreement with the computational reports for Y123 [22,29,47]. In addition, the experimental EFG at O2 and O3 sites of $YBa_2Cu_3O_{6.6}$ (Tab. 7) are equal, too. This means with reducing chain oxygens in $YBa_2Cu_3O_{7-\delta}$ compound, the number of doped holes at O2 and O3 sites reduces with the same value.

Table 7 shows that, the experimental amount of EFG at O2 site in Pr123 is very smaller than the EFG at O2 site in Y123, but the EFG at O3 site in Pr123 is equal to the EFG at O3 site in Y123. At first glance, the above observation suggests that Pr on Y site reduces only superconducting holes in O2 site and superconducting holes in O3 site do not change. The most famous theories that have been proposed to explain the suppression of superconductivity in Pr123 such as hole filling [52,53], Fehrenbacher and Rice model Hamiltonian [54], and Liechtenstein and Mazin calculations [7] argue that the substitution of Pr in Y site of Y123 compound reduces the superconducting holes in both O2 and O3 sites with the same manner. So, they imply that the EFG at O2 and O3 sites of Pr123 have almost to be the same and lower than the EFG at O2 and O3 sites of Y123 compound. Table 1 shows that the EFG at O2 and O3 sites in some calculations are lower than the experimental values for Y123 (Tab. 7), but in some other are not. So, some of our calculations are not consistent with the famous theories that mentioned in above. However, in all of our calculations, the EFG at O2 and O3 sites are almost equal. So, this aspect of all of our calculations is consistent with the famous theories that mentioned in above but, inconsistent with the experiment [46]. The most important question that must be answered is why the EFG at O2 site of Pr123 is unexpectedly lower than O3 site in experiment. It seems some defects could be responsible which we discuss about it below.

Table 12. The calculated EFG (V_{zz}) in units of 10^{21} V m^{-2} and asymmetry parameter η at O2 and O3 sites of $Pr(BaPr)Cu_3O_7$ in LSDA.

	$O2'$	$O3'$	$O2\frac{1}{2}$	$O3\frac{1}{2}$
EFG	5.9	6.0	5.0	4.9
η	0.2	0.2	0.3	0.3

There are some evidences that some defects may exist in the Pr123 sample that has been used in ^{17}O NMR spectroscopy in reference [46]. The transitions from the O(1) site (oxygen of chain) has not been observed in ^{17}O NMR spectroscopy in Pr123 [46]. This confirms the structural disorder of oxygens in the Cu-O chains of Pr123 sample that has been used in reference [46]. In addition, the unusual unspliting of central transition and low frequency satellites of O2 and O3 in reference [46] may also be related to the effects of some defects in CuO_2 planes. As has been mentioned in reference [45], high quality Pr123 crystals with a convenient size for NMR experiment ($\geqslant$10 mg) are still very difficult to prepare. For example, there is a probability that some other impurities such as Al from Al_2O_3 crucible contaminates the Cu1 sublattices and strongly influences the oxygen distribution [45]. In addition, Pr atoms can dissolve on Ba site in Pr123 samples [15]. Since Pr and Ba atoms have almost the same neutron-scattering lengths [55] and both Pr and Ba are atoms with almost similar high nuclear charges, neutron and X-ray scattering do not easily distinguish between Ba and Pr atoms [15]. Some indirect observations show that there are more than 0.23 Pr on Ba site (Pr_{Ba})/unit-cell in non-superconducting Pr123 samples [15]. Moreover, it has been shown that with increasing x in $Gd(Ba_{2-x}Pr_x)Cu_3O_{7-\delta}$ compound, the O5 occupation increases and for an x_c, the superconductor-insulator transition occurs [56-58]. So, the Pr_{Ba} mis-substitutions, which produce some oxygen disorders, can also be responsible for nonsuperconductivity and other unusual behaviors of conventional Pr123 samples.

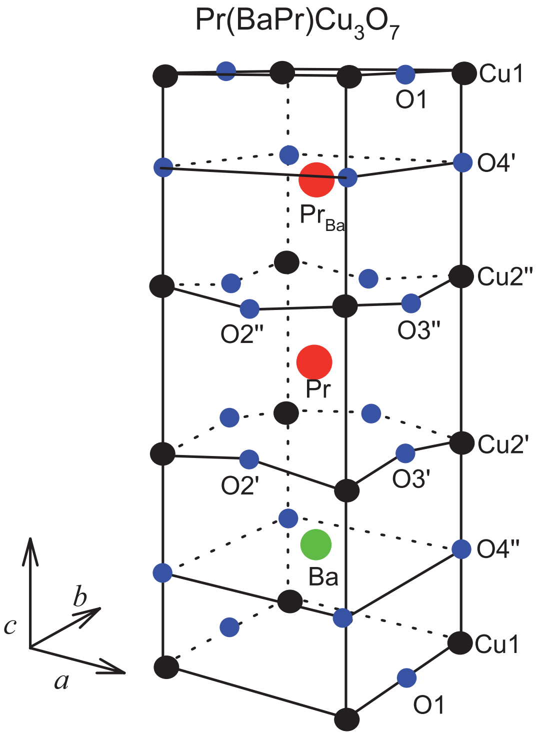

Fig. 2. The unit cell of Pr(BaPr)Ba$_2$Cu$_3$O$_7$.

As we have indicated in our last band structure calculation [9], Pr$_{Ba}$ mis-substitution reduces metallic (superconducting) character of perfect Pr123 samples and can be responsible for the suppression of metallic and superconducting characters of Pr123 samples. In [9] we have used an extreme case in which one Pr atom was replaced at one of the Ba sites in the unit cell of Pr123. The unit cell of this case (Pr(BaPr)Cu$_3$O$_7$ case) was shown in Figure 2. The effects of Pr$_{Ba}$ mis-substitution (Pr(BaPr)Cu$_3$O$_7$) on the EFG and η at O2 and O3 sites were reported in Table 12. Replacing Pr on Ba site breaks the inversion symmetry so, two O2 (O3) atoms in the unit cell of Pr123 are not equivalent and they are labeled with O2′ (O3′) and O2′ (O3′) in Figure 2. In this calculation, the LSDA was used and all of the computational parameters were the same as the Pr123 case. By comparison of Table 12 with case 1 in Table 1 (Pr123-LSDA case) we understand that Pr$_{Ba}$ mis-substitution obviously reduces the EFG at both O2 and O3 sites of Pr123. Decreasing the EFG at O2 and O3 sites means reducing superconducting holes at O2 and O3 sites. Therefore, our calculations prove that Pr$_{Ba}$ mis-substitution can be responsible for the suppression of superconductivity in Pr123 sample. In spite of this, in Table 12 the values corresponding to O2 sites are almost equal to the values of O3 one. So, our simplified mis-substitution calculation cannot explain the experimental smallness of the EFG at O2 site in comparison with O3 site.

Our mis-substitution calculation was very simplified. It has experimentally been shown [56–58] with increasing Pr on Ba site, O4 atoms migrate from their sites and the O5 site occupation increases. It is very probable that the unusual behaviors of the experimental EFG at O2 and O3 sites of Pr123 (and disappearance of the transitions from the O1 site in ^{17}O NMR spectroscopy [46]) is related to such defects. For more investigation, some other calculations that contain complicated disorders of Oxygen atoms in addition of Pr$_{Ba}$ mis-substitution are required. This needs very large supercells with huge computational cost.

At the end of this section some points should be mentioned. 1) It is not clear that the unusual behavior of the EFG at O2 and O3 sites is only corresponding to the specific nonsuperconducting Pr123 sample that has been used in [46] or it is a common behavior for all nonsuperconducting Pr123 samples that were carefully prepared by the conventional methods. In addition, the EFGs for unconventional superconducting Pr123 samples [11,12] have not been reported, yet. So, we strongly recommend that the EFG at O2 and O3 sites would be measured for various Pr123 samples. 2) In some references the U parameters for $3d$ or $4f$ orbitals of some compounds were calculated with the first principle calculations. One of them is the constrained local density approximation (CLDA) approach [60,61]. By this method the U is calculated from the total energy variation with respect to the occupation number of the localized orbitals. A further improvement of this method has recently been proposed [62,63]. Another method is based on the random phase approximation (RPA) [64,65]. It has been realized that these two methods of calculating the U (RPA and CLDA) do not yield the same results [66]. Significant discrepancy particularly towards the end of $3d$ series has recently been reported in [66]. So, the first principle methods have significant discrepancy yet and we have not calculated the U values first principally and used it as an external parameter. Using of U parameter as an external parameter is not unusual in LSDA+U calculations [20,36], and for our goal in this report is convenient. In this paper, we have tried to know that if LSDA+U calculations could produce the observed experimental EFG at Cu and especially O sites of nonsuperconducting Pr123 samples simultaneously. So, performing many calculations with various sets of U_{Cu1}, U_{Cu2}, and U_{Pr} is enough for our goal and we do not need exact values of three U parameters by the first principle calculations.

Conclusions

The EFG and asymmetry parameter η at all oxygen and copper sites of the PrBa$_2$Cu$_3$O$_7$ system were calculated using the FP+(L)APW+lo method [25,26]. To describe the exchange and correlation interactions the LSDA+U [32–34] was employed for Pr($4f$) and Cu($3d$) orbitals. The screened coulomb parameters U_{Pr}, U_{Cu1}, and U_{Cu2} were used as the external parameters and the effects of changing these parameters on the EFGs and ηs were investigated. The calculated EFGs for Pr123 in [5] were compared with our results. The EFG results of our LSDA case (case 1) are in good agreement with the EFG results of similar LSDA case (itinerant case) of reference [5]. Using U for $Pr(4f)$ orbitals and increasing U_{Pr} from zero to 0.74 Ry, the calculated EFG approaches to 3+ case in reference [5]. In addition, the calculated EFG results were compared with the experimental values. The most important point which was deduced from this comparison is that the calculated EFG at O2 site is close to the EFG at O3 site at variance with the experimental finding for nonsuperconducting Pr123 samples. Using the partial charges of O2 and O3 sites it was indicated that with increasing superconducting holes in O2 and O3 sites the EFG at these sites increases and vice versa. Using the relation of EFG and superconducting holes at O2 and O3 sites it was discussed that the most famous theories which have been proposed to explain the suppression of superconductivity in perfect Pr123 system are not consistent with the large experimental difference between the EFG at O2 and O3 sites similar to our computational results. There are some evidences that nonsuperconducting Pr123 sample that has been used in ^{17}O NMR spectroscopy [46] has not been perfect and probably some defects are responsible for the large discrepancy between the EFG at O2 and O3 sites.

By replacing one Pr atom at one of the Ba sites in the unit cell of Pr123, it was shown that Pr_{Ba} mis-substitution reduces the superconducting holes in both O2 and O3 sites. This could be responsible for the suppuration of superconductivity in Pr123 sample. This simplified mis-substitution calculation can not explain the experimental smallness of the EFG at O2 site in comparison with O3 site. It has experimentally been shown [56] that with increasing Pr on Ba site, the O4 atoms migrate from their sites, and the O5 site occupation increases. It is very probable that the unusual behaviors of the experimental EFG at O2 and O3 sites of Pr123 are related to such defects. We strongly recommend the ^{17}O NMR spectroscopy would be repeated with various Pr123 samples and the EFG at O2 and O3 sites should be investigated accurately.

The authors acknowledge technical support and helpful discussions with P. Novak, S. Jalali, S.J. Hashemifar, H. Akbarzadeh, P. Blaha, S. Cottenier, and K. Jorisson. We would also like to thank the Abdus Salam International Center for Theoretical Physics (ICTP) for good hospitality during revising this article. The partial financial support by the research council of the University of Tehran is acknowledged.

References

1. M. Akhavan, Physica B **321**, 265 (2002)
2. B. Rupp, E. Pörschke, P. Meuffels, P. Allenspach, P. Fischer, Phys. Rev. B **40**, 4472 (1989)
3. G.Y. Guo, W.M. Temmerman, Phys. Rev. B **41**, 6372 (1990)
4. D.J. Singh, Phys. Rev. B **50**, 4106 (1994)
5. C. Ambrosh-Draxl, P. Blaha, K. Schwarz, J. Phys.: Condens. Matter **6**, 2347 (1994)
6. M. Biagini, C. Calandra, S. Ossicini, Phys. Rev. B **52**, 10468 (1995)
7. A.I. Liechtenstein, I.I. Mazin, Phys. Rev. Lett. **74**, 1000 (1995)
8. M.C. Qian, W.Y. Hu, Q.Q. Zheng, J. Appl. Phys. **85**, 4765 (1999)
9. V. Ghanbarian, M.R. Mohammadizadeh, Phys. Stat. Sol. (c) **3**, 3122 (2006)
10. K. Takenaka, Y. Imanaka, K. Tamasaku, T. Ito, S. Uchida, Phys. Rev. B **46**, 5833 (1992)
11. Z. Zou, J. Ye, K. Oka, Y. Nishihara, Phys. Rev. Lett. **80**, 1074 (1998)
12. F.M. Araujo-Moreira, P.N. Lisboa-Filho, A.J.C. Lanfredi, W.A. Ortiz, S.M. Zanetti, E.R. Leite, A.W. Mombru, L. Ghivelder, Y.G. Zhao, V. Venkatesan, J. Magn. Magn. Mater. **226**, 283 (2001)
13. H.A. Blackstead, J.D. Dow, Phys. Rev. B **51**, 11830 (1995)
14. H.A. Blackstead, J.D. Dow, D.B. Chrisey, J.S. Horwitz, M.A. Black, P.J. McGinn, A.E. Klunzinger, D.B. Pulling, Phys. Rev. B **54**, 6122 (1996)
15. H.A. Blackstead, J.D. Dow, I. Felner, W.B. Yelon, Phys. Rev. B **63**, 094517 (2001)
16. J.D. Dow, H.A. Blackstead, D.R. Harshman, Physica C **364**, 74 (2001)
17. J.D. Dow, D.R. Harshman, J. Phys. Chem. Solids **63**, 2309 (2002)
18. P. Hohenberg, W. Kohn, Phys. Rev. A **136**, 864 (1964)
19. W. Kohn, L.J. Sham, Phys. Rev. A **140**, 1133 (1965)
20. P. Blaha, K. Schwarz, P. Novak, Int. J. Quantum Chem. **101**, 550 (2005)
21. P. Blaha, K. Schwarz, P. Herzing, Phys. Rev. Lett. **54**, 1192 (1985)
22. K. Schwarz, C. Ambrosch-Draxl, P. Blaha, Phys. Rev. B **42**, 2051 (1990)
23. P. Dufek, P. Blaha, K. Schwarz, Phys. Rev. Lett. **75**, 3545 (1995)
24. M. Takigawa, P.C. Hammel, R.H. Heffner, Z. Fisk, K.C. Ott, J.D. Thompson, Phys. Rev. Lett. **63**, 1865 (1989)
25. E. Sjöstedt, L. Nordström, D.J. Singh, Solid State Commun. **114**, 15 (2000)
26. G.K.H. Medsen, P. Blaha, K. Schwarz, E. Sjöstedt, L. Nordström, Phys. Rev. B **64**, 195134 (2001)
27. K. Schwarz, P. Blaha, Comp. Mater. Sci. **28**, 259 (2003)
28. D. Singh, Phys. Rev. B **43**, 6388 (1991)
29. D.J. Singh, K. Schwarz, P. Blaha, Phys. Rev. B **46**, 5849 (1992)
30. M. Guillaume, P. Allenspach, J. Mesot, B. Roessli, U. Staub, P. Fischer, A. Furrer, Z. Phys. B **90**, 13 (1993)
31. A.T. Boothroyd, J. Alloy. Compd. **303**, 489 (2000)
32. A.I. Liechtenstein, V.I. Anisimov, J. Zaanen, Phys. Rev. B **52**, R5467 (1995)
33. M.T. Czyzyk, G.A. Sawatzky, Phys. Rev. B **49**, 14211 (1994)
34. A.G. Petukhov, I.I. Mazin, L. Chioncel, A.I. Lichtenstein, Phys. Rev. B **67**, 153106 (2003)
35. J.P. Perdew, Y. Wang, Phys. Rev. B **45**, 13244 (1992)
36. P. Mohn, C. Persson, P. Blaha, K. Schwarz, P. Novak, H. Eschrig, Phys. Rev. Lett. **87**, 196401 (2001)
37. V.I. Anisimov, O. Gunnarsson, Phys. Rev. B **43**, 7570 (1991)
38. M. Biagini, C. Calandra, S. Ossicini, Phys. Rev. B **54**, 1404 (1996)

39. J.J. Yu, A.J. Freeman, R. Podloucky, P. Herzig, P. Weinberger, Phys. Rev. B **43**, 532 (1991)
40. G. Hilscher, E. Holland-Moritz, T. Holubar, H.D. Jostarndt, V. Nekvasil, G. Schaudy, U. Walter, G. Fillion, Phys. Rev. B **49**, 535 (1994)
41. A.T. Boothroyd, S.M. Doyle, R. Osborn, Physica C **217**, 425 (1993)
42. K. Nehrke, M.W. Pieper, T. Wolf, Phys. Rev. B **53**, 1 (1996)
43. K. Nehrke, M.W. Pieper, Phys. Rev. Lett. **76**, 1936 (1996)
44. A.P. Reyes, D.E. Maclaughlin, M. Takigawa, P.C. Hammel, R.H. Heffner, J.D. Thompson, J.E. Crow, A. Kebede, T. Mihalisin, J. Schwegler, Phys. Rev. B **42**, 2688 (1990)
45. M.W. Pieper, F. Wiekhorst, T. Wolf, Phys. Rev. B **62**, 1392 (2000)
46. Y.H. Co, H.K. Kweon, H.C. Lee, Physica C **244**, 357 (1994)
47. C.O. Rodriguez, R. Weht, N.E. Christensen, Physica C **282**, 1621 (1997)
48. M. Guillaume, P. Allenspach, W. Henggeler, J. Mesot, B. Roessli, U. Staub, P. Fischer, A. Furrer, V. Trounov, J. Phys.: Condens. Matter **6**, 7963 (1994)
49. V.I. Anisimov, *Strong Coulomb Correlation in Electronic Structure Calculations* (CRC, 2000)
50. M. Cyrot, D. Pavuna, *Introduction to Superconductivity and High-T_c Materials* (World Scientific Publishing Co. Pte. Ltd., 1992)
51. Y. Yoshinari, H. Yasuoka, Y. Ueda, K. Koga, K. Kojuge, J. Phys. Soc. Jpn. **59**, 3698 (1990)
52. A. Matsuda, K. Kinoshita, T. Ishii, H. Shibata, T. Watanabe, T. Yamada, Phys. Rev. B **38**, 2910 (1988)
53. A.P. Goncalves, I.C. Santos, E.B. Lopes, R.T. Henriques, M. Almeida, M.O. Figueiredo, Phys. Rev. B **37**, 7476 (1988)
54. R. Fehrenbacher, T.M. Rice, Phys. Rev. Lett. **70**, 3471 (1993)
55. V.S. Sears, Neutron News **3**, 26 (1992)
56. M.R. Mohammadizadeh, M. Akhavan, Phys. Rev. B **68**, 104516 (2003)
57. M.R. Mohammadizadeh, M. Akhavan, Eur. Phys. J. B **33**, 381 (2003)
58. M.R. Mohammadizadeh, M. Akhavan, Eur. Phys. J. B **42**, 321 (2004)
59. M.J. Stevenson, C.H. Townes, Phys. Rev. **107**, 635 (1957)
60. O. Gunnarsson, O.K. Andersen, O. Jepsen, J. Zaanen. Phys. Rev. B **39**, 1708 (1989)
61. V.I. Anisimov, J. Zaanen, O.K. Andersen, Phys. Rev. B **44**, 943 (1991)
62. I.V. Solovyev, M. Imada, Phys. Rev. B **71**, 045103 (2005)
63. M. Cococcioni, S. de Gironcoli, Phys. Rev. B **71**, 035105 (2005)
64. M. Springer, F. Aryasetiawan, Phys. Rev. B **57**, 4364 (1998)
65. F. Aryasetiawan, M. Imada, A. Georges, G. Kotliar, S. Biermann, A.I. Lichtenstein, Phys. Rev. B **70**, 195104 (2004)
66. F. Aryasetiawan, K. Karlsson, O. Jepsen, U. Schönberger, Phys. Rev. B **74**, 125106 (2006)